

# Implementation of channel-routing routines in the Water Erosion Prediction Project (WEPP) model\*

Li Wang<sup>†</sup>    Joan Q. Wu<sup>‡</sup>    William J. Elliot<sup>§</sup>    Shuhui Dun<sup>¶</sup>    Sergey Lapin<sup>||</sup>  
Fritz R. Fiedler<sup>\*\*</sup>    Dennis C. Flanagan<sup>††</sup>

## Abstract

The Water Erosion Prediction Project (WEPP) model is a process-based, continuous-simulation, watershed hydrology and erosion model. It is an important tool for water erosion simulation owing to its unique functionality in representing diverse landuse and management conditions. Its applicability is limited to relatively small watersheds since its current version does not simulate flow in permanent channels. In this study we developed a channel-routing module to simulate water flow in a permanent channel network. The module can utilize two methods: numerical kinematic-wave method and Muskingum-Cunge method. Results showed that, for appropriate temporal and spatial discretizations, both numerical solutions compared well with analytical solution of kinematic wave equations for simplified cases; otherwise, numerical dissipation from the kinematic wave solution, and numerical dispersion from the Muskingum-Cunge solution would occur.

## 1 Introduction.

Water resources are critical to a nation's security [15]. The quantity and quality of surface water resources depends on watershed attributes such as climate, geology, and topography, and watershed conditions affected by vegetation and human and natural disturbances [10]. Watersheds are frequently managed to ensure that runoff from the watershed meets conditions

suitable for downstream beneficial uses. One of the techniques used for watershed management is to model the effect of human disturbances on water quantity and quality, and to compare the results associated with different management practices. A "model" is a mathematical or qualitative representation of nature. It involves an understanding of the analysis area, including the identification of the important features and processes, such as topography, soil properties, vegetation, and climate as well as their interactions. Models provide answers to a variety of management questions, e.g., "what watershed changes are anticipated as a result of proposed fuel management activities?" [8].

A number of streamflow models have been developed [3]. Some perform better in predicting flows for larger channels over longer time steps (e.g., annual, long-term average), while others may be more suitable for smaller spatial scale and shorter time steps (e.g., seconds or minutes) [4].

The Water Erosion Prediction Project (WEPP) model is a process-based, continuous-simulation, watershed hydrology and erosion prediction model. The model inputs include climate, structure of hillslopes and channels, physical properties of hillslopes and channels (topography, geometry, geology), and, landuse, vegetation, and management practices. WEPP has been applied to agricultural and forested lands to simulate runoff and sediment yield from small watersheds. The model has been shown to be adequate in simulating daily water balance, including soil water content and streamflow [7], [27], [23].

Presently, the applicability of WEPP is limited to relatively small watersheds (<260 ha) since it does not simulate flow in permanent channels [9]. In WEPP, as summarized in [1], channel runoff is estimated using two options: the modified rational method used in the Erosion Productivity Impact Calculator (EPIC) model [24], and the regression equation used in the Chemicals, Runoff, and Erosion from Agricultural Management Systems (CREAMS) model [12]. Preliminary studies showed that WEPP could properly simulate daily water balance, but tended to over-predict peak

\*Supported by the USDA CSREES CEAP Grant (No. 2008-48686-04903).

<sup>†</sup>Department of Biological Systems Engineering, Washington State University, Pullman, WA.

<sup>‡</sup>Department of Biological Systems Engineering, Washington State University, Pullman, WA.

<sup>§</sup>Rocky Mountain Research Station, US Forest Service, Moscow, ID.

<sup>¶</sup>Department of Biological Systems Engineering, Washington State University, Pullman, WA.

<sup>||</sup>Department of Mathematics, Washington State University, Pullman, WA.

<sup>\*\*</sup>Department of Civil Engineering, University of Idaho, Moscow, ID.

<sup>††</sup>National Soil Erosion Research Laboratory, USDA Agricultural Research Service, West Lafayette, IN.

flow.

In a sediment erosion study in the North Caspar Creek Watershed, CA, a long-term US Forest Service experimental watershed, Conroy et al. [6] coupled WEPP with a hydrodynamic sediment transport model, CCHE1D [26]. The hillslope outputs from WEPP simulation were processed with an interface program and were then used as inputs to CCHE1D. Bdour and Papanicolaou [2] studied sediment erosion and transport in the Red River watershed, ID, by coupling WEPP with two hydrodynamic sediment transport models based on the hypsometric curve approach and the virtual velocity concept, respectively. The sediment from sub-watersheds simulated by WEPP was routed to the watershed outlet using the two sediment transport models. The additional data processing in coupling WEPP with streamflow and sediment transport models can be difficult for general users, which greatly limits the application of WEPP to larger watersheds.

Most current physically-based flood routing models are based on the St. Venant continuity and momentum equations [5]. The momentum equation includes force terms to describe water flow within a channel: local and convective acceleration forces, pressure force, gravitational force, and frictional force. Three types of hydraulic methods, which solve the St. Venant equations, have been used for streamflow routing. They are the dynamic wave, diffusion wave, and kinematic wave methods. The dynamic wave method includes all the momentum terms in the St. Venant equations. It is suitable for streams with gentle channel slopes and downstream controls (natural or man-made) where inertial and pressure forces and backwater effects are considered. The dynamic wave method is often numerically unstable and expensive to compute. The diffusion wave method neglects the local and convective acceleration terms in the St. Venant equations. The kinematic wave method is the simplest form of the St. Venant equations and has been widely used [19]. It neglects local and convective acceleration terms as well as the pressure force term, and only considers the gravitational and frictional force terms. The Muskingum-Cunge method numerically solves the kinematic wave equation, and considers both a storage and a transport concept. It may be considered as a hybrid approach [17].

In this study, a channel-routing module was developed and incorporated into the WEPP model (v2008.9). A numerical solution of the kinematic wave was implemented and verified against the analytical solution for a simplified case. Additionally, the Muskingum-Cunge method was implemented and its solution was compared with the analytical and numerical kinematic wave solutions. The modified WEPP model was applied to sim-

ulate watershed runoff from the North Fork of Caspar Creek Watershed, CA. In addition to computing daily water balance, the new channel routing module will route inflow from upstream and lateral flow through the stream banks to channel outlets at each specified time step.

## 2 Methods.

**2.1 Kinematic Wave Method.** Water flow in a one-dimensional channel can be described with the St. Venant equations [5], including a continuity equation and a momentum equation, as

$$(2.1) \quad \frac{\partial Q}{\partial x} + \frac{\partial A}{\partial t} = q,$$

and

$$(2.2) \quad \frac{1}{A} \frac{\partial Q}{\partial t} + \frac{1}{A} \frac{\partial}{\partial x} \left( \frac{Q^2}{A} \right) + g \frac{\partial y}{\partial x} - g(S_o - S_f) = 0$$

where  $A = A(x, t)$  and  $Q = Q(x, t)$  are the cross-sectional area and discharge of the channel flow, respectively,  $q = q(t)$  is lateral inflow,  $y = y(x, t)$  is depth of water,  $g$  is gravitational acceleration,  $S_o$  is the channel bed slope,  $S_f$  is the slope of the energy-grade line or friction slope,  $x$  is distance, and  $t$  is time.

For watershed modeling, the demand in data and computation is high due to the complexity of the highly dynamic and interactive hydraulic and hydrological processes at large scales. For water flow in a watershed where the slopes of stream channels tend to be steep and the gravitational force is dominant, the first three terms in equation (2.2) are negligible, and the gravity and friction forces are assumed to be balanced, leading to

$$(2.3) \quad S_o - S_f = 0.$$

The approach characterizing water flow by equations (2.1) and (2.3) is called the kinematic wave method. From equation (2.3),  $S_f = S_o$ . For uniform, turbulent channel flow, Manning's equation can be used to describe relationship between discharge and channel geometry [5]:

$$(2.4) \quad Q = \frac{S_o^{1/2}}{n} AR^{2/3}$$

where  $n$  is the Manning's roughness coefficient, and  $R$  is the hydraulic radius (ratio of the cross-sectional area to the wetted perimeter).

From equation (2.4), we have

$$(2.5) \quad \frac{\partial Q}{\partial t} = \frac{dQ}{dA} \frac{\partial A}{\partial t} = C_k \frac{\partial A}{\partial t}$$

where  $C_k = dQ/dA$  is the kinematic wave celerity. We present the calculation of  $C_k$  in the following for two different cross-sectional configurations of channels.

**2.1.1 Depth of water and kinematic wave celerity.** For a rectangular channel,

$$A = By, \quad R = \frac{By}{B + 2y}$$

where  $B$  is the channel bottom width, and  $y$  is the depth of water. We can then rewrite equation (2.4) as

$$(2.6) \quad Q = \frac{S_o^{1/2}}{n} By \left( \frac{By}{B + 2y} \right)^{2/3}.$$

For a known discharge  $Q_0$ ,  $y$  can be calculated using Newton's method [5].

The kinematic wave celerity  $C_k$  for a rectangular channel can be calculated from

$$(2.7) \quad C_k = \left( 1 + \frac{2B}{3(B + 2y)} \right) \frac{Q}{By}.$$

For a wide rectangular channel,  $B \gg y$ ,  $C_k$  can be simplified as [5], [25]

$$C_k = \frac{5Q}{3By}.$$

For a triangular channel,

$$A = sy^2, \quad R = \frac{sy}{2\sqrt{1 + s^2}}$$

where  $s$  is the inverse slope of the channel bank. We have

$$y = \left( \frac{A}{s} \right)^{1/2}, \quad R = \frac{s \left( \frac{A}{s} \right)^{1/2}}{2\sqrt{1 + s^2}},$$

and (as in Ponce [17])

$$(2.8) \quad Q = \frac{S_o^{1/2}}{n} A \frac{(sA)^{1/3}}{2^{2/3}(1 + s)^{1/3}} \\ = \frac{S_o^{1/2}}{2^{2/3}n} \left( \frac{s}{1 + s^2} \right)^{1/3} A^{4/3}.$$

For a triangular channel and a known  $Q_0$ ,  $y$  can be directly calculated from the following equation

$$(2.9) \quad y = \frac{2^{1/4} (1 + s^2)^{1/8} (nQ_0)^{3/8}}{S_o^{3/16} s^{5/8}}.$$

The kinematic wave celerity for a triangular channel can be derived from equation (2.8) as [17], [20]

$$(2.10) \quad C_k = \frac{4Q}{3sy^2}.$$

**2.1.2 Analytical method.** Combined with Manning's equation (2.4), equation (2.1) can be solved analytically. For a given discharge  $Q$  at the channel inlet, its kinematic wave celerity can be calculated using equations (2.7) and (2.10) for a rectangular and a triangular channel, respectively. Its travel time  $t$  to the outlet is [5]

$$(2.11) \quad t = \frac{L}{C_k}$$

where  $L$  is the channel length.

**2.1.3 Finite difference method.** With

$$\frac{\partial Q}{\partial t} = \frac{dQ}{dA} \frac{\partial A}{\partial t} = C_k \frac{\partial A}{\partial t},$$

eliminating  $A$  from equation (2.1), we obtain

$$(2.12) \quad \frac{\partial Q}{\partial x} + \frac{1}{C_k} \frac{\partial Q}{\partial t} = q.$$

The kinematic wave equations were solved by a finite difference method. Using a linear implicit scheme [5], we can express the partial differential equation (2.12) as

$$(2.13) \quad \frac{Q_{i+1}^{j+1} - Q_i^{j+1}}{\Delta x} + \frac{1}{C_k} \frac{Q_{i+1}^{j+1} - Q_{i+1}^j}{\Delta t} = \bar{q}$$

where  $i$  and  $j$  refer to the spatial and temporal nodes, respectively,  $Q_i^j = Q(i\Delta x, j\Delta t)$ ,  $\Delta x$  is the spatial increment, and  $\Delta t$  is the time step, and

$$\bar{q} = \frac{q_{i+1}^j + q_{i+1}^{j+1}}{2}.$$

In assessing and calibrating the channel-routing model, a user can define the time step  $\Delta t$  and space step  $\Delta x$  to test their effects on numerical dissipation and dispersion. In this study, we set  $\Delta t$  as one tenth of the weighted average  $t_c$  for all hillslopes to maintain appropriate temporal resolution, with defined upper and lower bounds. For the kinematic wave method,  $\Delta x$  for each channel is calculated based on the peak inflow and the Courant-Friedrichs-Lewy (CFL) condition to minimize the dissipation effect [5], [21]. The Courant number was assumed equal to or slightly less than 1, or  $\Delta x \geq C_{k, peak} \Delta t$ , where  $C_{k, peak}$  was calculated following equation (2.7) for a rectangular channel or (2.10) for a triangular channel using the peak inflow discharge.

$C_k$  in equation (2.13) can be estimated the same way as  $C_{k, peak}$  using the average discharge  $\bar{Q}$ :

$$\bar{Q} = \frac{Q_{i+1}^j + Q_i^{j+1}}{2}.$$

Solving equation (2.13) for the unknown  $Q_{i+1}^{j+1}$ , we obtain

$$(2.14) \quad Q_{i+1}^{j+1} = \frac{\frac{\Delta t}{\Delta x} Q_i^{j+1} + \frac{1}{C_k} Q_{i+1}^j + \Delta t \bar{q}}{\frac{\Delta t}{\Delta x} + \frac{1}{C_k}}.$$

It should be noted that, when the inflow hydrograph contains wave shocks, the numerical kinematic wave method may lead to mass balance and travel speed errors [14]; but under normal conditions, the mass balance errors may be neglected [11]. In our study, the daily inflow hydrograph from a hillslopes to a channel was simplified as a double-exponential function, the small mass-balance errors resulting from temporal and spatial discretization were further eliminated by assuming that the water storage in a channel cannot be negative, and the residual water that has not flowed out of the outlet of a channel remains as storage of the channel.

**2.2 Muskingum-Cunge Method.** The Muskingum method calculates channel outflow based on channel inflow and channel storage, with the assumption of a linear relationship of channel storage versus channel inflow and outflow [5], [17]. The Muskingum-Cunge method combines the Muskingum method with additional physical information, such as channel geometry and channel flow, and matches the numerical diffusion with the hydraulic diffusion of the channel flow [17]. The unknown discharge  $Q_{i+1}^{j+1}$  at  $(x_{i+1}, t_{j+1})$  can be calculated as [22]

$$(2.15) \quad Q_{i+1}^{j+1} = C_1 Q_i^{j+1} + C_2 Q_i^j + C_3 Q_{i+1}^j + C_4 \Delta x \bar{q}.$$

The coefficients  $C_1$ ,  $C_2$ ,  $C_3$ , and  $C_4$  in (2.15) are defined as

$$C_1 = \frac{\Delta t - 2KX}{2K(1-X) + \Delta t},$$

$$C_2 = \frac{\Delta t + 2KX}{2K(1-X) + \Delta t},$$

$$C_3 = \frac{2K(1-X) - \Delta t}{2K(1-X) + \Delta t},$$

and

$$C_4 = \frac{2\Delta t}{2K(1-X) + \Delta t}$$

where

$$K = \frac{\Delta x}{C_k},$$

and

$$X = \frac{1}{2} \left( 1 - \frac{Q_r}{BC_k S_o \Delta x} \right)$$

where  $B$  is the known channel width for a rectangular channel and  $B = 2sy$  for a triangular channel,  $Q_r$  is

the reference discharge, and  $C_k$  is estimated using  $Q_r$  from equation (2.7) for a rectangular channel or (2.10) for a triangular channel. For a greater computational efficiency,  $\Delta x$  may be specified as the length of the simulated channel [5], and  $Q_r$  as the peak inflow discharge. It has been shown that the mass balance errors from the Muskingum-Cunge method are negligible under normal conditions [18].

**2.3 Inflow hydrograph.** Within a stream network, the upstream end of a reach can receive inflow from one to three channels, or a single hillslope. Additional inflow can be from hillslopes on either side of the reach. Hillslope flux can include surface runoff and subsurface lateral flow. In the future, additional improvement may be made by modeling the ground-water base flow.

The daily hydrograph outputs from a WEPP hillslope simulation include the following parameters: hillslope runoff duration ( $t_d$ ), time of concentration ( $t_c$ ), peak runoff rate ( $q_p$ ), runoff volume ( $V$ ), and subsurface runoff volume ( $V_{sb}$ , with an assumed duration of 24 hours). These parameters define an input hydrograph of variable flow rate combining both hillslope surface runoff and subsurface lateral flow for each channel reach.

The current version of WEPP estimates the peak runoff rate for each channel reach as a fraction of peak precipitation intensity on the hillslopes [8]. Conroy et al. [6] used a linear equation for the rising limb of the hydrograph, and regression equations derived from observed data for the falling limb, considering  $V$  and  $t_c$  from the WEPP hillslope simulation outputs. In the present study, we used a double-exponential function defined from all of the WEPP daily hydrograph parameters (Figure 1) to describe a continuous hillslope surface flow hydrograph for channel routing. Such an approach was also used in WEPP for fitting rainfall intensity data [16]. The double-exponential function is given by

$$(2.16) \quad q_f(t) = \begin{cases} q_p e^{b(t-t_c)} & 0 \leq t \leq t_c \\ q_p e^{-d(t-t_c)} & t_c < t \leq t_d \end{cases}$$

where  $q_f(t)$  is the calculated runoff rate, and  $t_c$  is assumed to be the time that the peak runoff rate occurs. The coefficients  $b$  and  $d$  can be obtained using Newton's method with the assumption

$$q_f(0) = q_f(t_d)$$

and mass conservation

$$\int_0^{t_d} q_f(t) dt = V.$$

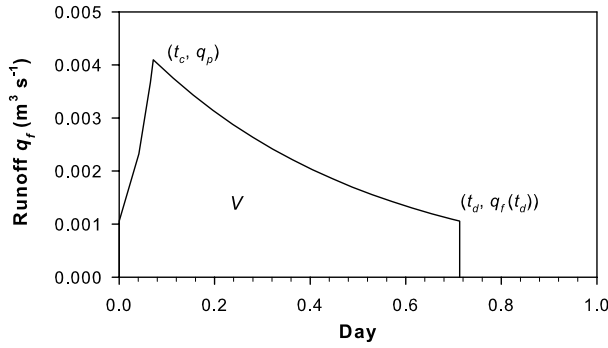


Figure 1: An example of the double-exponential function  $q_f(t)$  defined using the parameters from the WEPP daily hillslope surface runoff outputs, North Fork sub-watershed of Caspar Creek Watershed, January 14, 1995.  $t_c$ , time of concentration,  $t_d$ , runoff duration,  $q_p$ , peak runoff rate, and  $V$ , runoff volume.

**2.4 Case simulations.** For the purpose of model verification and assessment of model performance, we simulated water flow in a hypothetical channel network (Figure 2) using the channel-routing module. The channel network consisted of four rectangular open channels with triangular inflow hydrograph for channels 1–3.

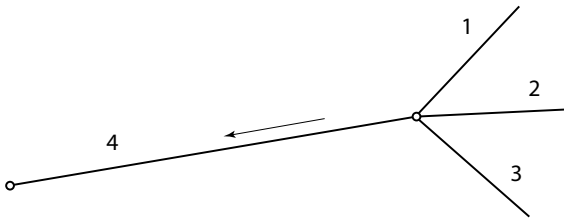


Figure 2: A hypothetical channel network, including four rectangular open channels, for the verification of the channel-routing module. The triangular inflow hydrographs for channels 1–3 were identical. The outflow hydrograph for channel 4 was calculated analytically and numerically as shown in Figure 3.

We then applied the modified WEPP model to the North Fork of Caspar Creek Watershed, CA. The Caspar Creek Experimental Watershed is located in the middle of Jackson Demonstration State Forest, south of Fort Bragg, CA. It has been studied for the effects of forest management on runoff and soil erosion since 1962 [13]. The North Fork drains an area of 473 ha (1.83 mi<sup>2</sup>). Gauging stations have been installed for 21 sites to monitor streamflow [13].

Except for the study by Conroy et al. [6] coupling

WEPP with the CCHE1D model to evaluate upland erosion and channel sediment transport, systematic simulation for overland and channel flow for this area is lacking. As in Conroy et al. [6], we discretized the North Fork sub-watershed of Caspar Creek Watershed into 88 hillslopes and 35 channels.

To compare the effects of time step and assess the differences in the analytical and numerical kinematic wave solutions as well as the Muskingum-Cunge method, we ran the WEPP model using time steps of 10 or 60 min in the two numerical methods. The simulation results were also compared with the observed hydrograph at the outlet of the North Fork sub-watershed of Caspar Creek watershed.

### 3 Results.

**3.1 Verification of kinematic wave and Muskingum-Cunge solution.** With an appropriate temporal and spatial discretization, the results from the numerical kinematic wave solution and the Muskingum-Cunge method compared well with the analytical kinematic wave solution (Figure 3).

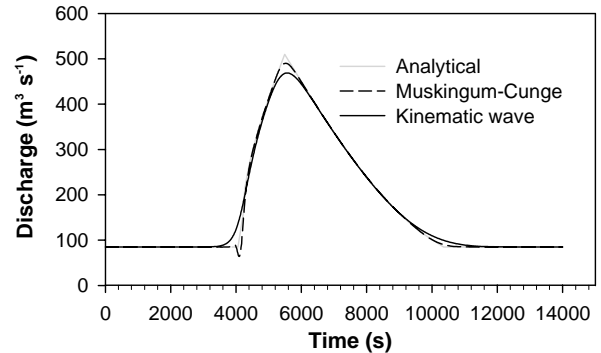


Figure 3: Comparison of analytical and numerical kinematic wave solutions and Muskingum-Cunge method for water flow out of channel 4 of the hypothetical channel network (Figure 2), using a spatial interval of 300 m and a time step of 10 s.

**3.2 Effects of  $\Delta x$  and  $\Delta t$  on numerical solutions.** The numerical kinematic wave method led to dissipation, or wave attenuation with time [21]. The dissipation increased with the size of temporal and spatial increments in this study, as reported in previous studies [5].

The numerical dissipation from the Muskingum-Cunge method was negligible. But numerical dispersion, i.e., waves with different wave lengths travel at different speeds [21], was observed if  $\Delta t$  was too small

for a selected  $\Delta x$ , or  $\Delta x$  was too large for a selected  $\Delta t$ . This was because parameter  $C_1$  in equation (2.15) would become negative, leading to decreased flow at the wave front (Figure 3).

**3.3 Application to North Fork of Caspar Creek Watershed, CA.** The simulated hydrograph by using the numerical kinematic wave solution with a 10-min time step (KW, 10 min) is shown in Figure 4. The results from the numerical kinematic wave solution with a 60-min time step (KW, 60 min), the Muskingum-Cunge method with a 10-min or 60-min time step (MC, 10 min and MC, 60 min, respectively) are shown as differences from this hydrograph (Figure 4). The additional rises or dips (usually at the beginning or end of a day) caused by using the KW, 60 min were mainly because of resolution difference. The results from the Muskingum-Cunge method yielded a slightly higher peak flow than the numerical kinematic wave solution, and showed some numerical dispersion. The numerical dispersion from using  $\Delta t = 60$  min was higher than using  $\Delta t = 10$  min.

The simulated daily peak flows by the kinematic wave and Muskingum-Cunge methods are shown in Figure 5. Compared with the CREAMS method in the original WEPP that led to high flow peaks, the kinematic wave and Muskingum-Cunge methods had lower peak flows.

The simulated hydrograph was also compared with observed streamflow data (Figure 6) for January 1995. The first simulated peak is lower than the observed, but the others are agreeable with the observed.

The total storage in all the channels upstream from the outlet of the North Fork Caspar Creek sub-watershed is usually smaller than the amount of daily inflow or outflow in January (Figure 7), because of the high velocity of water flow. During a dry season, surface-water storage in the sub-watershed may be larger than the amount of inflow or outflow (not shown). Figure 7 also indicates that the time of the largest storage may not coincide with the time of the largest flow event.

#### 4 Summary and Conclusions.

A channel-routing module was developed to simulate water flow in a channel network using either the numerical kinematic wave method or Muskingum-Cunge method. With appropriate temporal and spatial discretization, both numerical solutions compared well with the analytical solution of kinematic wave equations for simplified cases. The kinematic wave method was more robust even for nonlinear waves, but the resultant numerical dissipation increased with the sizes of

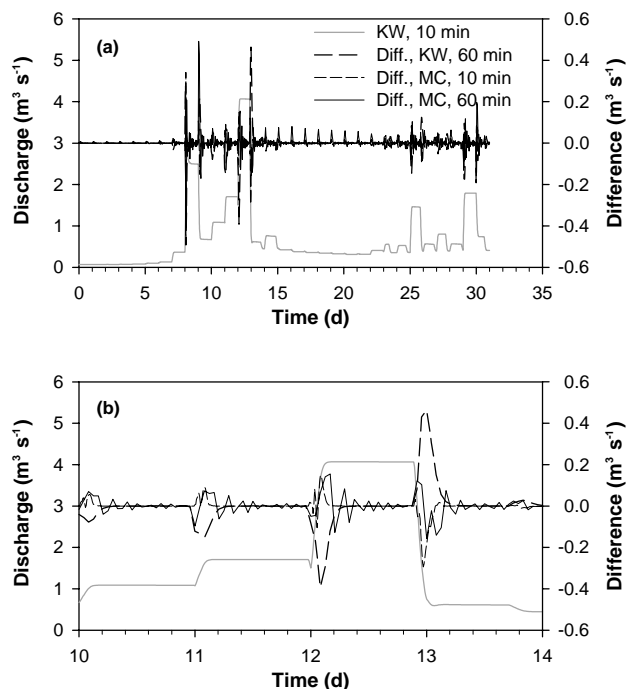


Figure 4: Simulated hydrograph by the numerical kinematic wave solution using a time step of 10 min (KW, 10 min), and discharge differences by using the numerical kinematic wave solution with a 60-min time step (Diff., KW, 60 min), and the Muskingum-Cunge method with a 10-min or 60-min time step (Diff., MC, 10 and 60 min, respectively), for the North Fork of Caspar Creek, (a) January 1995, (b) a blowup of January 11–14, 1995.

temporal and spatial discretization. The Muskingum-Cunge method was computationally more efficient, and the resultant peak attenuation was smaller. From this point of view, we suggest the Muskingum-Cunge method to be used for calculating peak flows in erosion estimation, as in the WEPP model. Future work includes code implementation to minimize numerical dispersions in the Muskingum-Cunge method, and testing the channel-routing routines newly incorporated in the WEPP model with streamflow data from different geographic localities.

#### References

- [1] J. C. Ascough, C. Baffaut, M. A. Nearing, and D. C. Flanagan, *Watershed model channel hydrology and erosion processes*, chap. 13, in D. C. Flanagan and M. A. Nearing, eds., *Technical Documentation: USDA-Water Erosion Prediction Project (WEPP)*, USDA-

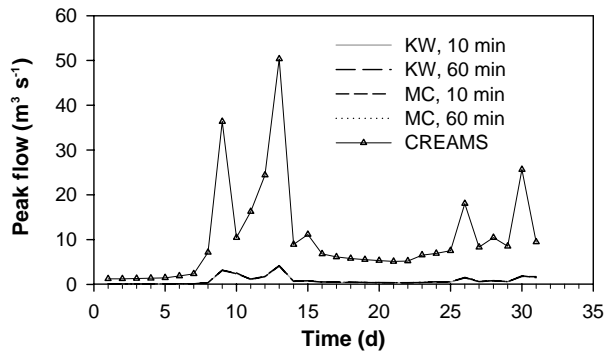


Figure 5: Simulated peak flows for the North Fork of Caspar Creek, January 1995. KW, kinematic wave, MC, Muskingum-Cunge, CREAMS, Chemicals, Runoff, and Erosion from Agricultural Management Systems.

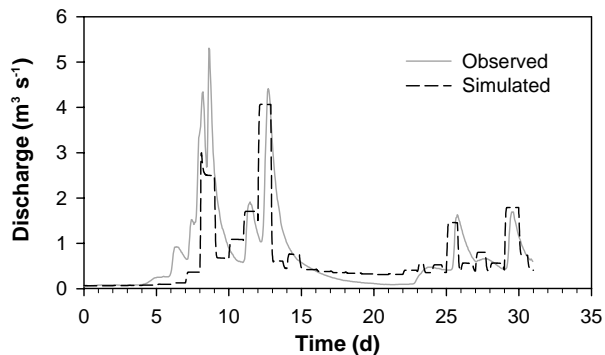


Figure 6: Comparison of simulated and observed hydrographs for the North Fork of Caspar Creek, January 1995.

ARS Natl. Soil Erosion Res. Lab., West Lafayette, IN, 1995.

- [2] A. Bdour and T. Papanicolaou, *The coupling of a two-dimensional hydrodynamic/sediment routing model with an upland watershed erosion model in a mountain watershed, Red River, Idaho*, presented at The 3<sup>rd</sup> Int. Conf. Water Resour. Arid Environ. the 1<sup>st</sup> Arab Water Forum, Riyadh, Saudi Arabia, 2008.
- [3] D. K. Borah and M. Bera, *Watershed-scale hydrologic and nonpoint-source pollution models: Review of mathematical bases*, Trans. ASAE, 46 (2003), pp. 1553–1566.
- [4] ———, *Watershed-scale hydrologic and nonpoint-source pollution models: Review of applications*, Trans. ASAE, 47 (2004), pp. 789–803.
- [5] V. T. Chow, D. R. Maidment, and L. W. Mays, *Applied Hydrology*, McGraw-Hill, New York, 1988.
- [6] W. J. Conroy, R. H. Hotchkiss, and W. J. Elliot, *A coupled upland-erosion and instream hydrodynamic-sediment transport model for evaluating sediment trans-*

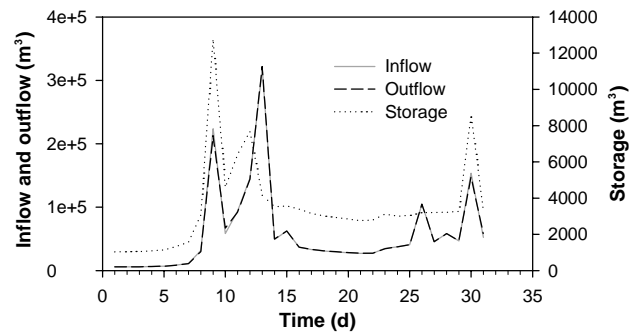


Figure 7: Daily water balance of the North Fork of Caspar Creek, January 1995, from the WEPP channel routing.

*port in forested watersheds*, Trans. ASABE, 49 (2006), pp. 1713–1722.

- [7] S. Dun, J. Q. Wu, W. J. Elliot, P. R. Robichaud, D. C. Flanagan, J. R. Frankenberger, R. E. Brown, and A. C. Xu, *Adapting the Water Erosion Prediction Project (WEPP) model for forest applications*, J. Hydrol., 466 (2009), pp. 46–54.
- [8] W. Elliot, K. Hyde, L. MacDonald, and J. McKean. *Tools for analysis*, in W. J. Elliot and L. J. Audin, eds., (2007, January 19—last update). DRAFT Cumulative Watershed Effects of Fuels Management in the Western United States. Available Online: <http://forest.moscowfls.wsu.edu/engr/cwe/> [Accessed Sep. 2009].
- [9] D. C. Flanagan and S. J. Livingston, eds., *USDA-Water Erosion Prediction Project: User Summary*, NSERL Rep. No. 11. USDA-ARS Natl. Soil Erosion Res. Lab., West Lafayette, IN, 1995.
- [10] D. D. Fangmeier, W. J. Elliot, S. R. Workman, R. L. Huffman, and G. O. Schwab. *Soil and Water Conservation Engineering*, 5<sup>th</sup> ed., Clifton Park, NY, 2006.
- [11] D. Gasiorowski and R. Szymkiewicz, *Mass and momentum conservation in the simplified flood routing models*, J. Hydrol., 346 (2007), pp. 51–58.
- [12] W. G. Knisel, ed., *CREAMS: A Field-scale model for chemicals, runoff, and erosion from agricultural management systems*, USDA Cons. Res. Rpt. No. 26. Washington, D.C., 1980.
- [13] E. Keppeler, J. Lewis, and T. Lisle, *Effects of forest management on streamflow, sediment yield, and erosion, Caspar Creek Experimental Watersheds*, in K. G. Renard, S. A. McElroy, W. J. Gburek, H. E. Canfield, and R. L. Scott, eds., 1<sup>st</sup> Interagency Conf. Res. Watersheds, Benson, AZ, 2003.
- [14] R. J. LeVeque, *Numerical Methods for Conservation Laws*, 2<sup>nd</sup> ed., Birkhäuser Verlag, 1992.
- [15] W. C. Lowdermilk, *Conquest of the Land through Seven Thousand Years*, Washington, D.C., Gov. Print. Off., 1953.

- [16] A. D. Nicks, L. J. Lane, and G. A. Gander, *Weather generator*, chap. 2, in D. C. Flanagan and M. A. Nearing, eds., Technical Documentation: USDA-Water Erosion Prediction Project (WEPP), USDA-ARS Natl. Soil Erosion Res. Lab., West Lafayette, IN, 1995.
- [17] V. M. Ponce, *Engineering Hydrology, Principles and Practices*, Prentice Hall, Englewood Cliffs, NJ, 1995.
- [18] V. M. Ponce and P. V. Chaganti, *Variable-parameter Muskingum-Cunge method revisited*, *J. Hydrol.*, 162 (1994), pp. 433–439.
- [19] V. P. Singh, *Kinematic wave modelling in water resources: A historical perspective*, *Hydrol. Process.*, 15 (2001), pp. 671–706.
- [20] M. H. Tewold and J. C. Smithers, *Flood routing in ungauged catchments using Muskingum methods*, *Water SA*, 32 (2006), pp. 379–388.
- [21] J. W. Thomas, *Numerical Partial Differential Equations: Finite Difference Methods*, Springer-Verlag, New York, 1995.
- [22] G. -T. Wang, C. Yao, C. Okoren, and S. Chen, *4-Point FDF of Muskingum method based on the complete St Venant equations*, *J. Hydrol.*, 324 (2006), pp. 339–349.
- [23] J. D. Williams, S. Dun, D. S. Robertson, J. Q. Wu, E. S. Brooks, D. C. Flanagan, and D. K. McCool, *WEPP simulations of dryland cropping systems in small drainages of Northeastern Oregon*, *J. Soil Water Conserv.*, 65 (2010), pp. 22–33.
- [24] J. R. Williams, *The Erosion-Productivity Impact Calculator (EPIC) model: A case history*, *Philos. Trans. Biol. Sci.*, 329 (1990), pp. 421–428.
- [25] T. S. W. Wong, *Comparison of celerity-based with velocity-based time-of-concentration of overland plane and time-of-travel in channel with upstream inflow*, *Adv. Water Resour.*, 26 (2003), pp. 1171–1175.
- [26] W. Wu and D. A. Vieira, *One-dimensional channel network model CCHE1D, ver. 3.0: Technical manual*, Tech. Rep. No. NCCHE-TR-2002-1, Natl. Cent. Comput. Hydrosci. Eng., Univ. Miss., 2002.
- [27] J. X. Zhang, J. Q. Wu, K. Chang, W. J. Elliot, and S. Dun, *Effects of DEM resolution on WEPP hydrologic and erosion simulation: A case study of two forest watersheds in northern Idaho*, *Trans. ASABE*, 52 (2009), pp. 447–457.